

Clinoptilolite, kieselguhr and α -alumina supported nano-nickel boride catalysts for the production of high purity p-aminophenol through p-nitrophenol hydrogenation: a comparative study

Firouzeh Taghavi, Cavus Falamaki, Alimemad Shabanov, Leila Bairami & Mina Seyyedi

Reaction Kinetics, Mechanisms and Catalysis

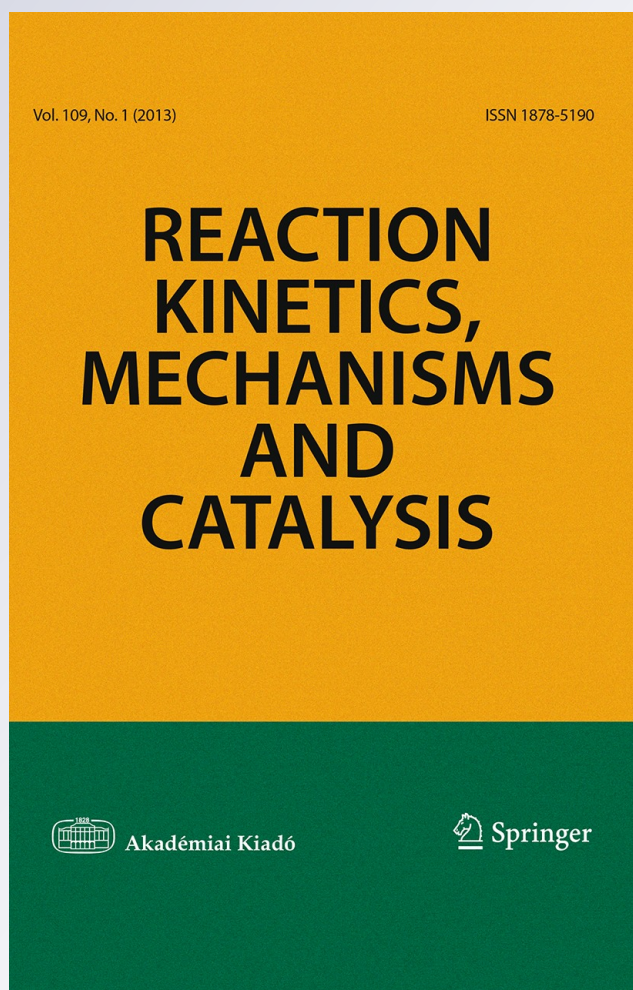
ISSN 1878-5190

Volume 109

Number 1

Reac Kinet Mech Cat (2013) 109:91-104

DOI 10.1007/s11144-013-0539-4



Your article is protected by copyright and all rights are held exclusively by Akadémiai Kiadó, Budapest, Hungary. This e-offprint is for personal use only and shall not be self-archived in electronic repositories. If you wish to self-archive your article, please use the accepted manuscript version for posting on your own website. You may further deposit the accepted manuscript version in any repository, provided it is only made publicly available 12 months after official publication or later and provided acknowledgement is given to the original source of publication and a link is inserted to the published article on Springer's website. The link must be accompanied by the following text: "The final publication is available at link.springer.com".

Clinoptilolite, kieselguhr and α -alumina supported nano-nickel boride catalysts for the production of high purity *p*-aminophenol through *p*-nitrophenol hydrogenation: a comparative study

Firouzeh Taghavi · Cavus Falamaki ·
Alimemad Shabanov · Leila Bairami · Mina Seyyedi

Received: 19 September 2012 / Accepted: 21 January 2013 / Published online: 1 February 2013
© Akadémiai Kiadó, Budapest, Hungary 2013

Abstract The morphology of supported nickel boride nanoparticles depends strongly on the exposed surface cation exchange property of the support. Despite having a substantially higher loading of nickel boride, the α -Al₂O₃ supported catalyst exhibits a significantly lower catalytic activity for the hydrogenation of *p*-nitrophenol. Use of a supporting material like clinoptilolite allows the re-use of the catalyst up to three times. However, the catalytic activity decreases after each hydrogenation process. Unsupported nickel boride and α -Al₂O₃ supported nickel boride result in unwanted trace impurities in the final *p*-aminophenol crystalline product. Such impurities are absent using clinoptilolite and kieselguhr supports.

Keywords Nickel boride · Clinoptilolite · Kieselguhr · *p*-Nitrophenol · *p*-Aminophenol · Hydrogenation

F. Taghavi · A. Shabanov
Research Institute of Geotechnological Problems of Oil, Gas and Chemistry, Azerbaijan State Oil Academy, Baku, Azerbaijan

F. Taghavi · L. Bairami · M. Seyyedi
Research and Development Department, Chlor Pars Co., P.O. Box 51335-1717, Tabriz, Iran

C. Falamaki (✉)
Chemical Engineering Department, Amirkabir University of Technology, P.O. Box 15875-4413, Tehran, Iran
e-mail: c.falamaki@aut.ac.ir

C. Falamaki
Petrochemical Center of Excellence, Amirkabir University of Technology, P.O. Box 15875-4413, Tehran, Iran

Introduction

p-Aminophenol (PAP) is a well known intermediate reagent and has a wide application in the production of acetaminophen (AC) and dye stuffs [1, 2]. Competition in the commercial production of amino compounds is high, and a successful process must produce a good yield of pure product in a simple and economical manner [3].

The direct catalytic hydrogenation of nitrophenols is an industrially important process for the production of aminophenols [4, 5]. Catalytic hydrogenation is the cheapest possible way to reduce *p*-nitrophenol (PNP) in the presence of nickel catalysts. The amorphous Ni–B alloy catalyst synthesized by the chemical reduction method is superior to normal nickel-based catalysts (such as Raney Nickel) in activity, selectivity [6–8] and sulfur-poison-resistive properties [9, 10].

Among various amorphous alloy catalysts, the Ni-based type has been studied most thoroughly [11]. Nevertheless, their industrial application is still severely limited due to several reasons: (a) Poor thermal stability (b) Heavy mass loss during separation from the product and (c) The existence of unacceptable trace impurities in the final product. The first case is due to the thermodynamically metastable amorphous structure of the catalyst. Crystallization can occur spontaneously during the reaction, even at very low temperatures, resulting in an abrupt decrease in activity. The second case is due to the nano-structure of the nickel boride catalyst. Upon attrition of the particles during the reaction and product separation steps, a large portion of the catalyst is lost as very fine particles after the separation of the liquid and solid phases. To obtain an economic process compatible with industrial operation, it is necessary to be able to recycle the catalyst. The third case is extremely important, especially when the final PAP is used for the production of AC. Incidentally; AC is an analgesic and must be very pure, without any colored impurities because of its use as a drug. Therefore, the appearance and quality of PAP as a starting material is an important factor in attaining pure AC and reduction of production and purification costs. In this direction, PNP should be completely converted to PAP. Any residual PNP is not allowed because it may degrade to nitro-cathecol, dihydroxynitrobenzene, hydroquinone and benzoquinone during PAP storage. Impure samples are dark colored due to the presence of chemicals like quinhydrone.

Recently, many new supported nano-amorphous Ni–B alloys with better thermo-mechanical stability have been prepared by the chemical reduction method, e.g. Ni–B/SiO₂ [6, 12–14] Ni–B/Al₂O₃ [15, 16], Ni–B/mesoporous silica [17], Ni–B/SBA-15 [18], Ni–B/MCM-41 [13], Ni–B/amine-modified silica nano-spheres [19], Ni–B/borohydride exchange resin [20], Ni–B/activated carbon [21] and Ni–B/HMCM-22 zeolite [22]. Some of them showed higher activity and selectivity in catalytic hydrogenation of compounds [16, 21, 22].

Synthetic zeolite 4A, perlite and silica gel supported nickel boride was prepared by Acosta et al. [23] and used in the hydrogenation of nitrobenzene. The characterization of the as-prepared catalyst was poor and the synthesis method of the catalyst was not effective for industrial application. In the meantime, the activity of the catalyst in hydrogenation reaction was very low.

Rahman and Jonnalagadda [24] investigated the hydrogenation of nitro aromatic compounds (mainly PNP) with sodium borohydride in the presence of nickel/SiO₂ catalyst. Nickel boride was formed during the hydrogenation reaction.

Wen et al. [25] prepared polymer supported nano Ni–B and applied it in the reduction of nitro aromatic compounds (especially PNP) using hydrazine hydrate. The catalyst was recycled two times. Hydrazine is highly toxic and dangerously unstable. The application of the mentioned material in the industrial synthesis of PAP is questionable because of detrimental effects in AC production. Such reagents are subject to severe limitations for application in plant scale reactions because of safety and handling considerations. When hydrogenation reactions cease to be practical and enter the stage of industrial development, the cost of the hydrogenation process becomes highly important.

Liu et al. [26] synthesized Ni–B/boehmite, Ni–B/ γ -Al₂O₃ and Ni–B/Al₂O₃·xH₂O and used for the direct reduction of PNP to PAP. As-synthesized catalysts have been characterized only by TEM and XRD. XRD patterns of the supported catalysts were mainly belonging to the supports owing to the amorphous nature of nickel boride. Ni–B/boehmite had superior activity, selectivity and could be recycled three times.

Based on the literature cited, a comparative investigation of a number of the most potential candidates for supports of nickel boride catalysts is still lacking for specific hydrogenation reactions. These include natural zeolites, diatomaceous earth and different alumina phases other than γ -Al₂O₃. On the other hand, and to the knowledge of the authors of this work, no report regarding the exclusion of unwanted trace impurities due to interaction of the support with the reacting system has been reported so far.

This work consists of a comparative study of the physico-chemical characteristics of nickel boride catalysts supported on clinoptilolite, kieselguhr and α -alumina. The chemical aspect considers the behavior of the aforesaid composite catalysts in the PNP to PAP hydrogenation reaction. The re-usability of the catalysts is investigated. The effect of the support on product impurity is considered for the first time. It will be shown that trace impurities show themselves also in the abrupt change of PAP solid crystals morphology. This effect will be accordingly explained.

Experimental

Materials

Synthesis grade nickel chloride, caustic soda, hydrochloric acid and sodium borohydride were supplied by Merck. α -Al₂O₃ and hydrogen were provided by Iran alumina Co. (Iran) and Chlor Pars Co. (Iran), respectively. A natural Iranian clinoptilolite zeolite was used. Ethanol, kieselguhr and PNP were purchased from Nasr Co. (Iran), Zarrin Khak Ghaen (Iran) and Anhui Bayi Co. (China), respectively.

The catalysts were prepared by the impregnation method by dissolving 1.78 g nickel chloride in 25 ml distilled water and adding it to 5 g support (zeolite, kieselguhr or α -alumina) and stirring for more than 12 h using a magnetic stirrer at room temperature. The mixture was dried by heating at 94 °C under stirring. The

nickel precursor was reduced by adding 0.05 M NaBH₄ solution dropwise. The sodium borohydride solution was prepared by dissolving 0.57 g sodium borohydride in 25 ml solution containing 0.05 M HCl or distilled water. The B/Ni molar ratio was 1/1. During the reduction reaction, the temperature was kept at 94 °C and the reaction mixture was stirred gently. The resulting supported nickel boride catalyst was filtered and washed thoroughly with distilled water until the pH of the filtrate reached a value of 7. The synthesized catalyst was kept under ethanol before use in the activity tests.

Unsupported nickel boride was synthesized through the dropwise addition of the same sodium borohydride aqueous solution to the nickel chloride solution according to the method described in our previous paper [27].

Activity tests

Liquid-phase hydrogenation of PNP was performed at 2.5 MPa hydrogen pressure and 80 °C in a 400 ml stainless steel autoclave, in which zeolite, kieselguhr or α -alumina supported nickel boride catalysts, 3.5 g PNP and 25 ml ethanol were well mixed. Details about the reaction system may be found elsewhere [27]. The reaction system was stirred vigorously (46 rpm) to eliminate mass transfer resistance as explained in our previous work [27]. The hydrogenation reaction was performed at 80 °C and 2.5 MPa. The extent of the reaction was monitored by measuring the total pressure with reaction time. The reaction mixture was filtered to separate the catalyst. The zeolite supported catalysts were separated from the reaction solution, thoroughly washed with ethanol and maintained under ethanol for further reactions (recycling of the catalyst). The filtrate was cooled at 0 °C for the crystallization of the product. PAP was filtered and dried in an oven at 60 °C. The PAP products were analyzed with a GC (Agilent 7890 Series, USA) equipped with a FID detector and an auto-sampler. Chromatographic separations were performed at 325 °C using an Agilent 19091j-413 30 m \times 320 μ m \times 0.25 μ m column and nitrogen as carrier gas at a flow rate of 1 ml min⁻¹.

Catalyst characterization

FTIR spectra were recorded with a Tensor 27 (Bruker) spectrometer. All the spectra were measured at room temperature after the samples were pressed to KBr wafers. X-ray powder diffraction patterns were obtained on a Siemens D5000 powder diffractometer with Cu K α radiation. The morphology and particle size of the samples were investigated using a field emission scanning electron microscope (S-4160, Hitachi). BET surface area of the samples was measured by N₂ adsorption on an Autosorb-1 (Quanta Chrome) apparatus. ICP analysis was performed using an Integra XL (GBC) apparatus.

Results and discussion

Fig. 1 shows the XRD patterns of the supported nickel boride catalysts. The XRD pattern of an unsupported nickel boride catalyst has been included for comparison.

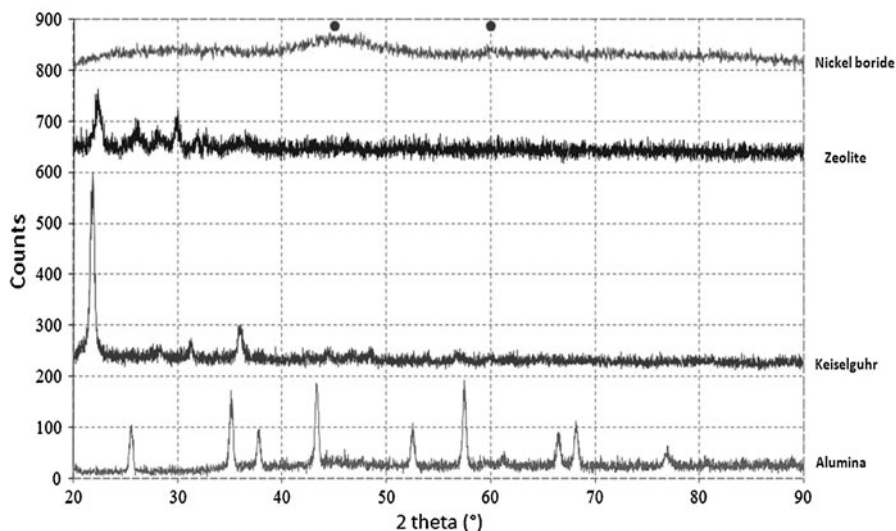


Fig. 1 XRD patterns of the supported and the parent nickel boride catalysts (filled circle: Ni_2B crystalline phase)

Nickel boride has an amorphous structure and the two main “hills” indicated in Fig. 1 may be attributed to the Ni_2B phase [27]. The characteristic peaks of nickel boride may not be discerned in the XRD patterns of the supported samples. This is probably due to the very low amount of nickel boride present and/or a very good dispersion of nickel boride catalyst on the supports. It should be noted that according to the XRD analysis, the kieselguhr sample consists solely of a crystalline crystalalite phase.

Fig. 2 shows the FTIR patterns of the supports and supported nickel boride catalysts. The main difference between the α -alumina and α -alumina supported nickel boride samples concerns the wavelength range of $500\text{--}1,500\text{ cm}^{-1}$ (Fig. 2b, c). The sharp and strong peaks at $1,266$ and 919 cm^{-1} are attributed to BO_3 groups and that at 612 cm^{-1} is assigned to BO_4 groups [28].

A comparison of the spectra belonging to the zeolite support and nickel boride/zeolite catalyst (Fig. 2d, e) reveals the presence of BO_3 groups ($1,500\text{--}1,400\text{ cm}^{-1}$), which is characterized by short and strong B–O chemical bonds. The weak double peaks centered at ca. $1,453\text{ cm}^{-1}$ and a single peak at $1,200\text{ cm}^{-1}$ are attributed to anti-symmetrical stretching vibrations of $\nu_3(\text{BO}_3)$ modes of B–O bonds in BO_3 groups [28].

FTIR spectra of kieselguhr and nickel boride on kieselguhr samples are presented in Fig. 2f, g. The weak peak observed at around $1,450\text{ cm}^{-1}$ on the Ni–B/kieselguhr spectrum is attributed to anti-symmetrical stretching vibration of BO_3 groups as for the nickel boride/zeolite catalyst. In summary, it may be stated that the α -alumina supports contain substantially more nickel boride entities compared to kieselguhr and zeolite supported catalysts.

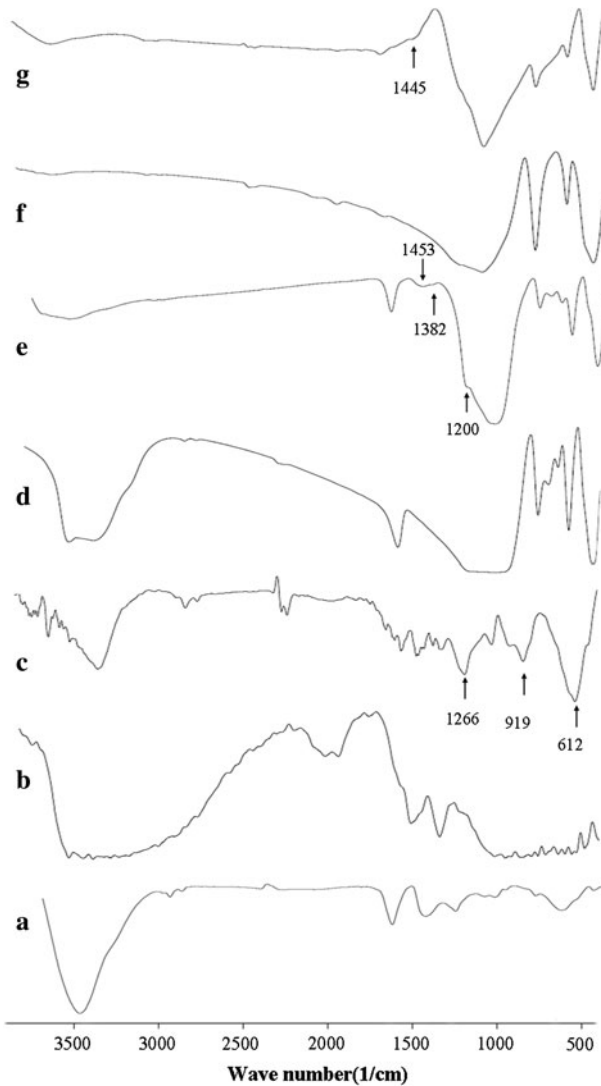


Fig. 2 FTIR patterns of (a) nickel boride (b) α -alumina (c) α -alumina supported catalyst (d) clinoptilolite zeolite (e) clinoptilolite supported catalyst (f) kieselguhr and (g) kieselguhr supported catalyst

Catalytic activity is a surface effect connected to the available and exposed surface area of the catalyst [29]. The specific surface area of the supports and supported catalysts is summarized in Table 1. The specific surface area of α - Al_2O_3 is inherently low ($7.5 \text{ m}^2\text{g}^{-1}$) and increases by a factor of ca. 4 upon impregnation with nickel boride particles. Kieselguhr is also subjected to a significant increase of surface area (more than fivefold) after the coating process ($17\text{--}89 \text{ m}^2\text{g}^{-1}$). The clinoptilolite zeolite undergoes a rather small increase in surface area (more than twofold).

In each case, the increase in surface area is due to the addition of nanosized nickel boride particles to the support materials. It goes without saying that nanoparticles have inherently high surface areas due to their relatively small size, which are substantially larger than the specific surface areas of the supports used in this work. This is confirmed by referring to the FESEM pictures shown in Fig. 3a–h. It is observed that unsupported nickel boride appears as detached nanosized, quasi-spherical particles on the exposed surfaces of clinoptilolite and kieselguhr supports. The nanoparticles exhibit an approximately sharp mono model distribution in the case of kieselguhr, with an average particle diameter of around 30 nm. The nickel boride particles on the zeolite show a relatively broad size distribution, in the range of 20–150 nm. The smaller increase in the specific surface area for the zeolite upon loading with the catalyst is attributed to the mentioned size distribution difference.

The morphology of the nickel boride particles on α -Al₂O₃ support is not quasi-spherical and represents a foamy structure. At this point, it is interesting to consider the morphology of unsupported nickel boride particles. They exhibit a foamy structure, too. Therefore, it seems that upon coating, a buildup of nickel boride particles produced in the liquid phase on the α -alumina support takes place. The mechanism of nanoparticle formation on the exposed surface of clinoptilolite and kieselguhr is indeed different. Clinoptilolite and kieselguhr both have cation exchange capacities (CEC). The CEC of the clinoptilolite sample is ca. 200 meq/100 g and kieselguhr around 56 meq/100 g. Upon treatment with NiCl₂ solution, Ni²⁺ cations undergo an ion exchange reaction with the exchangeable cations on clinoptilolite and kieselguhr surface. Hence, the initial available surface area of these materials becomes saturated with covalently attached Ni²⁺ cations. This is not the case for α -alumina which has negligible exchange capacity. It is presumed that, upon contact with NaBH₄ solution, the surface exchangeable Ni²⁺ cations of clinoptilolite and kieselguhr undergo an ion exchange reaction with the Na⁺ cations in the solution just adjacent to the solid surface. The released Ni²⁺ cation then undergoes a redox reaction with the BH₄⁻ anion. This phenomenon results in the creation of seed points for nickel boride entities on the surface, ultimately leading in the creation of the nanosized detached nickel boride particles with quasi-spherical morphology. In the case of α -alumina, the Ni²⁺ cations are mainly provided by the solution (dissolved NiCl₂ in the NaBH₄ solution) and presumably, are first produced in the solution. This explains the ‘build-up’ mechanism cited above for nickel boride particle formation on α -Al₂O₃.

The activity and selectivity of metal borides can be altered significantly by varying the amount of metal-associated boron [30–32]. Table 2 shows the ICP

Table 1 Specific surface area of the supports and catalyst/support samples

Support	Specific surface area (m ² g ⁻¹)	Catalyst/support	Specific surface area (m ² g ⁻¹)
Clinoptilolite	40	Ni-B/zeolite	88
Kieselguhr	17	Ni-B/kieselguhr	89
α -Al ₂ O ₃	5–10	Ni-B/ α -Al ₂ O ₃	31

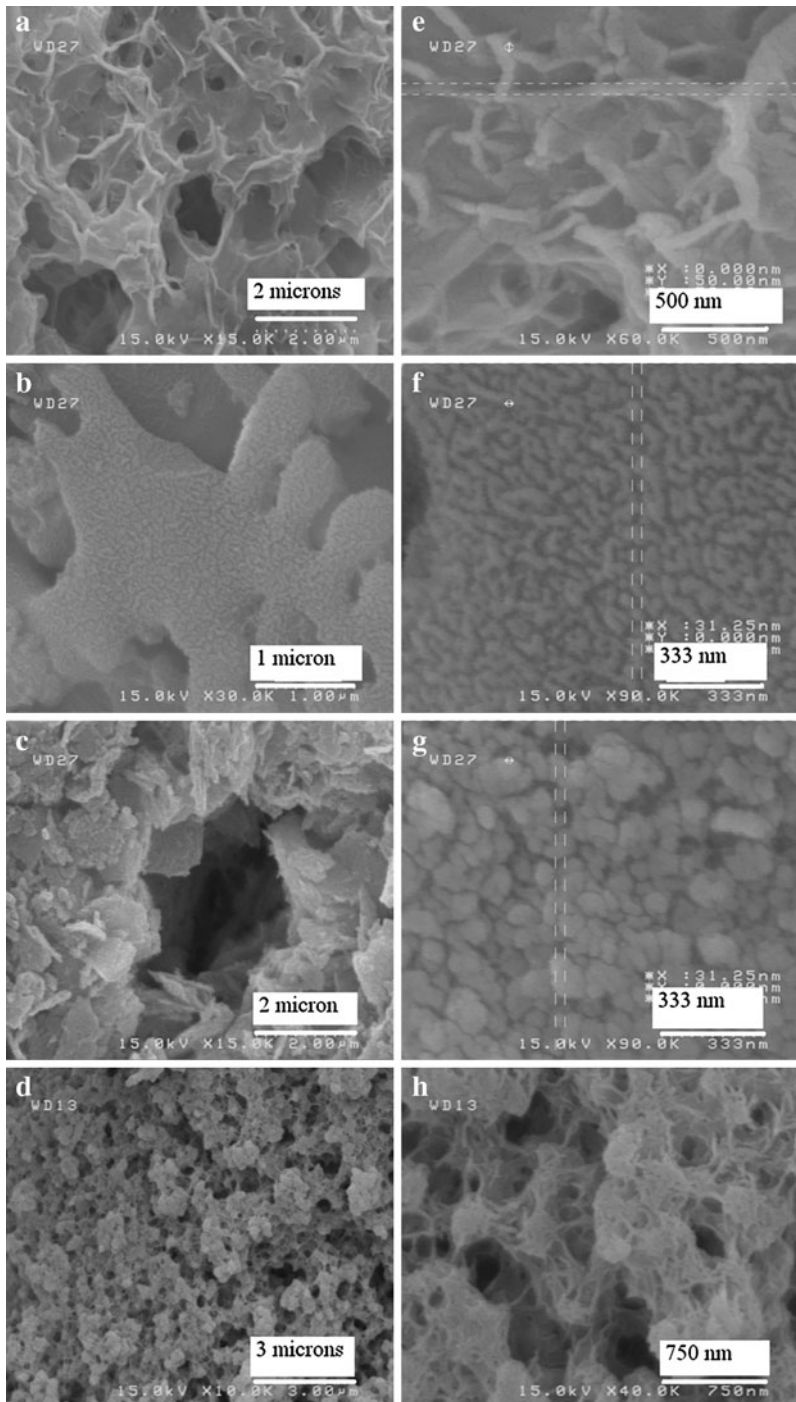


Fig. 3 FESEM pictures of α -alumina supported nickel boride (a and e), kieselguhr supported nickel boride (b and f), clinoptilolite supported nickel boride (c and g) and unsupported nickel boride (d and h)

analysis for the supported catalysts samples. While the content of nickel and boron is substantially higher for α -alumina, it is approximately the same for the zeolite and kieselguhr supports. The corresponding chemical formula of the catalyst is Ni_xB , where x varies from 1.9 to 2.5. This is in accordance with the FTIR and FESEM results, which showed a higher loading of nickel boride for the α -alumina support.

Fig. 4 shows the kinetic behavior of the supported catalysts for the PNP hydrogenation reaction for an initial pressure of 25 bar. It is observed that kieselguhr and clinoptilolite show a similar trend, while the reaction is significantly slower in the case of α -alumina supported catalyst. The initial rate is ca. $-0.142 \text{ bar min}^{-1}$ for clinoptilolite and kieselguhr and $-0.10 \text{ bar min}^{-1}$ for α - Al_2O_3 . Recall that the nickel content of the latter catalyst is about 2.5 times that of nickel boride/clinoptilolite or nickel boride/kieselguhr catalysts. The lower activity of the α -alumina supported catalyst is mainly attributed to the lower specific surface and foamy morphology of the nickel boride particles formed on the α - Al_2O_3 support. Actually, catalytic activity is a strong function of catalyst chemical composition (core and surface) and morphology (determining the specific surface area of the active site) at the same time. For clinoptilolite and kieselguhr supported catalysts, the high surface area of the nickel boride particles compensates the lower

Table 2 ICP analysis of the supported catalysts

Catalyst/support	Nickel (wt%)	Boron (wt%)
Nickel boride/clinoptilolite	7.1	0.7
Nickel boride/kieselguhr	8.3	0.62
Nickel boride/ α -alumina	20.7	1.52

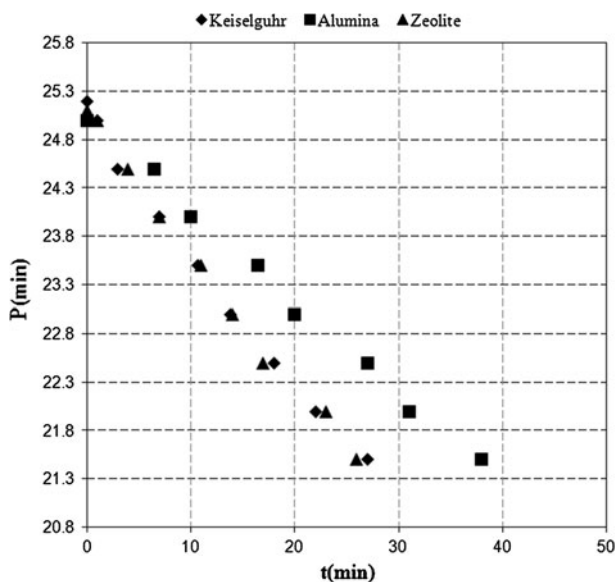


Fig. 4 Total pressure variation as a function of the hydrogenation reaction time

boron content (inherent catalytic activity) and, the activity is generally higher than for the alumina supported catalyst. As said before, the substantially lower surface area of the nickel boride foamy body is the main cause of the relatively lower activity, overshadowing the inherent higher activity due to higher boron content.

An important characteristic for supported catalysts is their re-usability for the same reaction process conditions. The clinoptilolite supported catalyst was recycled two times after completion of the reaction. The results are shown in Fig. 5. It is observed that the catalyst activity is highly reduced after each run. It should be noted that the unsupported nickel boride catalyst could only be used one time, while the supported one showed activity in the third run. The loss of activity after recycling is mainly attributed to the poisoning of the catalyst active sites by organic amines and oxygenated nitro compound, formation of complex compounds and dissolution of nickel during the reaction [33].

The clinoptilolite and kieselguhr supports exhibit a unique property which is very promising for their industrial applications. Fig. 6a–d show the GC analysis of the isolated and crystallized PAP final product. In the case of Fig. 6a, b, the reaction has been stopped at ca. 70 % conversion of PNP. For the latter figures, the first sharp peak on the left belongs to the PAP solvent used for the analysis. The peaks appearing ca. 3.03 min belong to PAP. The peaks appearing around 3.5 min belong to an acceptable impurity. It is noteworthy that the chromatogram of a high purity PAP sample provided from MERCK Co. also shows the same peak. However, the chromatogram due to the α -Al₂O₃ supported catalyst shows extra impurity peaks at 5.3 and 6.3 min. This is

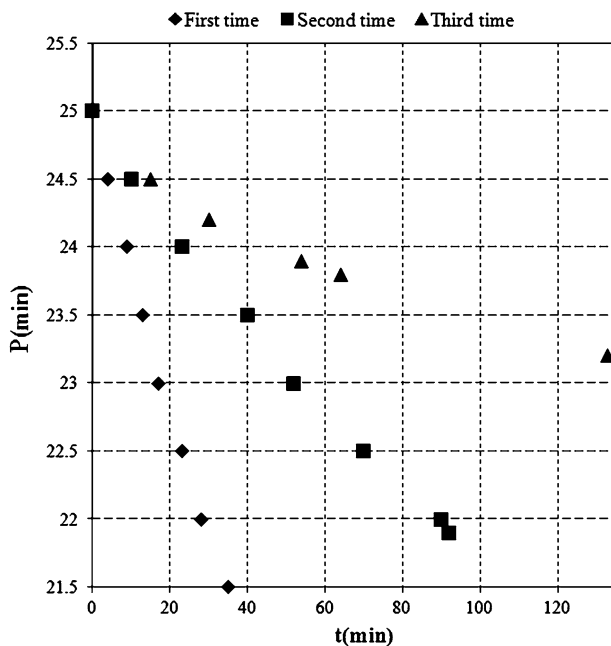


Fig. 5 Effect of clinoptilolite supported catalyst re-usage on pressure variation as a function of reaction time

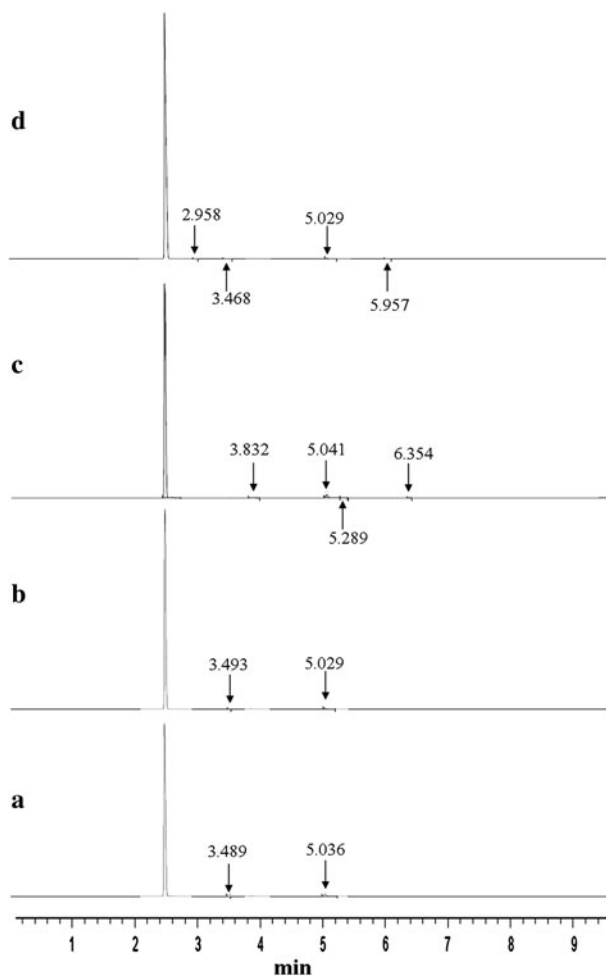


Fig. 6 GC chromatograms of the isolated PAP crystals produced using (a) kieselguhr supported catalyst (b) clinoptilolite supported catalyst (c) α -alumina supported catalyst and (d) unsupported nickel boride

while the pertaining product has an unacceptable brown appearance. The pattern due to the unsupported catalyst shows impurity peaks at 2.9 and 5.9 min. Trace impurities, and especially those changing the appearance of the PAP product, are not acceptable when the PAP product is going to be used in the production of dye stuffs and AC. The impurity compounds may be 4-nitrophenol, 4-aminophenol among others. As we could not identify them, it was not possible to quantify them. The main deduction at this stage is that clinoptilolite and kieselguhr supports are highly desired for their ability to eliminate such impurities in the final product. The authors of this work suppose that presumably the impurities do create during the hydrogenation reaction, but they are selectively adsorbed by the highly porous structure made available by the supports. Such a phenomenon has not been reported so far. As a concluding remark, it is interesting to consider the morphology of the final PAP crystals with and without the

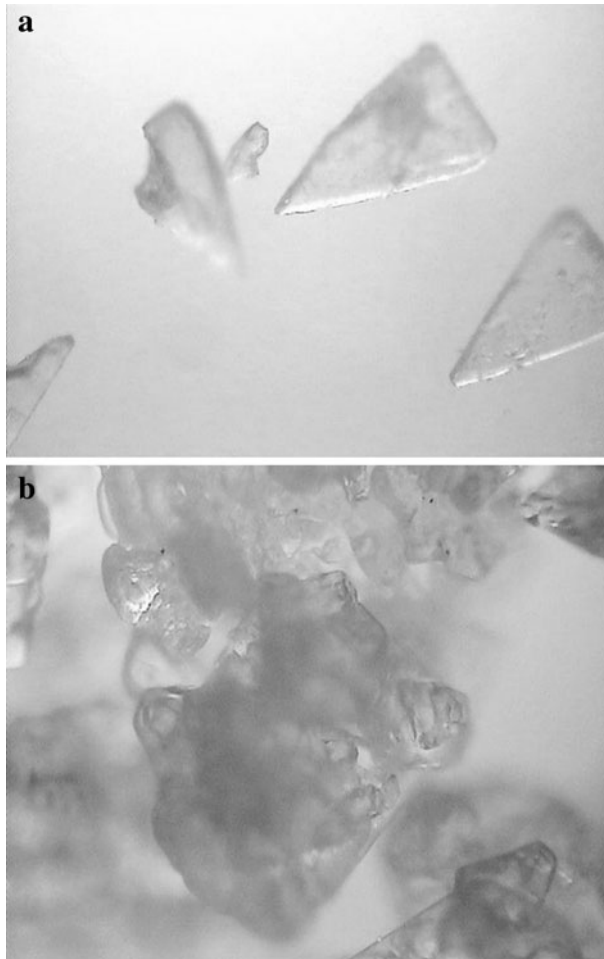


Fig. 7 Optical microscope pictures of PAP crystals obtained using **a** clinoptilolite supported catalyst and **b** unsupported catalyst

presence of the aforesaid impurities (Fig. 7a, b). It is clearly observed that in the absence of undesired impurities, the crystal assume a distinct mono-modal triangular flaky morphology (Fig. 7a). In the presence of these impurities, the crystals tend to have a multi-modal irregular morphology (Fig. 7b).

Conclusions

The morphology of supported nickel boride nanoparticles depends strongly on the exposed surface cation exchange property of the support. This allows a nucleation and growth mechanism of nickel boride particles on the exposed surface of the support in the case of clinoptilolite and kieselguhr materials. Creation of nickel boride nanoparticles on α - Al_2O_3 proceeds via a nucleation/growth process

originating in the adjacent liquid phase. This results in the “build-up” of bulky nickel boride particles on the support. FTIR and ICP analysis show a higher loading of the catalyst material on the support in the case of α -Al₂O₃.

Despite having a substantially higher loading of nickel boride, the α -Al₂O₃ supported catalyst has a significantly lower catalytic activity. This has been mainly attributed to the lower specific surface and foamy morphology of the nickel boride particles formed on the α -Al₂O₃ support. This is while nickel boride/clinoptilolite and nickel boride/kieselguhr show a similar catalytic activity. This is due to a similar loading and average particle size of the catalyst material on their exposed surfaces.

Use of a supporting material like clinoptilolite allows the re-use of the catalyst up to three times. However, the catalyst activity decreases after each hydrogenation process. The catalyst activity is reduced 3.6 folds after one run and 4.7 folds after the second run.

Unsupported nickel boride and α -Al₂O₃ supported nickel boride result in unwanted trace impurities in the final PAP crystalline product. Instead, such impurities are absent in the PAP product obtained using clinoptilolite and kieselguhr supported nickel boride catalysts. Presumably, the latter supports selectively adsorbed these impurities during the reaction.

Acknowledgments The authors would like to thank Chlor Pars Co. (Tabriz, Iran) for the partial financial support of the work.

References

1. Figueras F, Deshpande A, WO2009060050A2 (2009) Center National De La Recherche Scientifique (C.N.R.S)
2. Rode CD, Vaidya MJ, Chaudhari RV, US 6,403,833 (2002) Council of Scientific & Industrial Research (New Delhi, India)
3. Spiegler L, Woodbury NJ, US 2,947,781 (1960) E. I. du Pont de Nemours and Company
4. Studer M, Baumeister P, US 6,096,924 (2000) Novartis AG (Basel, Switzerland)
5. Ding J, Chen L, Shao R, Wu J, Dong W (2012) *Reac Kinet Mech Cat* 106:225–232
6. Xie SH, Li HX, Li H, Deng JF (1999) *Appl Catal A Gen* 189:45–52
7. Li HX, Xu YP, Li H, Deng JF (2001) *Appl Catal A Gen* 216:51–58
8. Li H, Li HX, Deng JF (2001) *Mater Lett* 50:41–46
9. Wang WJ, Li HX, Deng JF (2000) *Appl Catal A Gen* 203:293–300
10. Li HX, Li H, Dai WL, Qiao MH (2003) *Appl Catal A Gen* 238:119–130
11. Deng JF, Li H, Wang WJ (1999) *Catal Today* 51:113–125
12. Li H, Li HX, Dai WL, Deng JF (2001) *Appl Catal A Gen* 207:151–157
13. Wong ST, Lee JF, Chen JM, Mou CY (2001) *J Mol Catal A* 165:159–167
14. Wang WJ, Qiao MH, Li HX, Dai WL, Deng JF (1998) *Appl Catal A Gen* 168:151–157
15. Li J, Qiao MH, Deng JF (2001) *J Mol Catal A* 169:295–301
16. Zhang RB, Li FY, Shi QJ, Luo LT (2001) *Appl Catal A Gen* 205:279–284
17. Chen X, Wang S, Zhuang J, Qiao M, Fan K, He H (2004) *J Catal* 227:419–427
18. Chen XY, Hu HR, Liu B, Qiao MH, Fan KN, He HY (2003) *J Catal* 220:254–257
19. Chen Y, Kim H (2008) *Fuel Process Technol* 89:966–972
20. Choi J, Yoon NM (1996) *Tetrahedron Lett* 37:1057–1060
21. He YG, Qiao MH, Hu HR, Deng JF, Fan KN (2002) *Appl Catal A Gen* 228:29–37
22. Lu Y, Xiong ZT, Li JT, Lin JY (2002) *Catal Lett* 78:231–237
23. Acosta D, Martinez J, Carrera C, Erdmann E, Gonzo E, Destefanis H (2006) *Lat Am J Chem Eng Appl Chem* 36:317–320

24. Rahman A, Jonnalagadda SB (2008) *Catal Lett* 123:264–268
25. Wen HL, Yao KS, Zhang Y, Zhou ZM, Zhou Z, Kirschning A (2009) *Catal Commun* 10:1207–1211
26. Liu H, Deng J, Li W (2010) *Catal Lett* 137:261–266
27. Taghavi F, Falamaki C, Shabanov A, Bayrami L, Roumianfar A (2011) *Appl Catal A Gen* 407:173–180
28. Markova-Deneva I (2009) The global conference on micro manufacture, incorporating the 5th international conference on multi-materials micro manufacture (4M) and the 4th international conference on micro manufacture (ICOMM). In: *Proceedings of the Conference 4M/ICOMM*, p 263. doi: [10.1243/17547164C0012009052](https://doi.org/10.1243/17547164C0012009052)
29. Patel N, Patton B, Zanchetta C, Fernandes R, Guella G, Kale A, Miotello A (2008) *Int J Hydr Energy* 33:287–292
30. Okamoto Y, Fukino K, Imanaka T (1982) *J Catal* 74:173–180
31. Okamoto Y, Nitta Y, Imanaka T, Teranishi S (1979) *J Chem Soc Faraday Trans I(75)*:2027–2038
32. Okamoto Y, Matsunaga E, Imanaka T, Teranishi S (1982) *J Catal* 74:183–187
33. Du Y, Chen H, Chen R, Xu N (2006) *Chem Eng J* 125:9–14